Chemistry & Biology
Article

Rational Design of Small Molecule Inhibitors Targeting the Rac GTPase-p67^{phox} Signaling Axis in Inflammation

Emily E. Bosco,[1] Sachin Kumar,[1] Filippo Marchioni,[1] Jacek Biesiada,[2] Miroslaw Kordos,[2] Kathleen Szczur,[1] Jarek Meller,[2,3] William Seibel,[4] Ariel Mizrahi,[5] Edgar Pick,[5] Marie-Dominique Filippi,[1,*] and Yi Zheng[1,*]
[1]Division of Experimental Hematology and Cancer Biology
[2]Division of Biomedical Informatics
Children's Hospital Medical Center, Cincinnati, OH 45229, USA
[3]Department of Environmental Health
[4]Drug Discovery Center
University of Cincinnati, Cincinnati, OH 45237, USA
[5]Julius Friedrich Cohnheim Laboratory of Phagocyte Research, Department of Clinical Microbiology and Immunology, Sackler School of Medicine, Tel Aviv University, 69978 Tel Aviv, Israel
*Correspondence: marie-dominique.filippi@cchmc.org (M.-D.F.), yi.zheng@cchmc.org (Y.Z.)
DOI 10.1016/j.chembiol.2011.12.017

SUMMARY

The NADPH oxidase enzyme complex, NOX2, is responsible for reactive oxygen species production in neutrophils and has been recognized as a key mediator of inflammation. Here, we have performed rational design and in silico screen to identify a small molecule inhibitor, Phox-I1, targeting the interactive site of p67^{phox} with Rac GTPase, which is a necessary step of the signaling leading to NOX2 activation. Phox-I1 binds to p67^{phox} with a submicromolar affinity and abrogates Rac1 binding and is effective in inhibiting NOX2-mediated superoxide production dose-dependently in human and murine neutrophils without detectable toxicity. Medicinal chemistry characterizations have yielded promising analogs and initial information of the structure-activity relationship of Phox-I1. Our studies suggest the potential utility of Phox-I class inhibitors in NOX2 oxidase inhibition and present an application of rational targeting of a small GTPase-effector interface.

INTRODUCTION

Originally characterized in phagocytes, the multicomponent nicotinamide adenine dinucleotide phosphate (NADPH) oxidase NOX2 enzyme complex facilitates the production of reactive oxygen species (ROS) to mediate innate immunity. These oxygen species are generated from a superoxide anion (O^{2-}) that is produced by phagocytes in order to kill invading microorganisms (Bedard and Krause, 2007). In humans, mutations in any of the components of the NADPH oxidase complex can lead to chronic granulomatous disease (CGD), where the superoxide production defect results in a patient's inability to fight infection and in aberrant inflammation (Roos, 1994). This NADPH oxidase-dependent process has now been shown to occur in many different cell types for both host defense and intracellular signal transduction (Sundaresan et al., 1996; Takemura et al., 2010). Thus, beyond its role in pathologies of host defense, inappropriate regulation of the NADPH oxidase complex has been proposed to contribute to a multitude of inflammation-mediated disorders, including cancer, atherosclerosis, hypertension, chronic obstructive pulmonary disease (COPD), myocardial infarction, and stroke (Armitage et al., 2009; Bedard and Krause, 2007; Kleinschnitz et al., 2010; Williams and Griendling, 2007).

Because superoxide and secondary ROS can also cause tissue damage and initiate inflammatory responses, NADPH oxidase activity must be stringently regulated. Biochemical studies over the past two decades have identified a well-defined molecular mechanism of NOX2 regulation; its activation is dependent on a series of protein interactions that are initiated in the cytoplasm and translocate to the cell membrane for full NADPH oxidase complex activation. In the prototypical phagocytic superoxide production event, in response to inflammatory stimuli, four cytosolic proteins in the "regulatory complex," that is, Rac1/2, p47^{phox}, p67^{phox} and p40^{phox}, are translocated to the membrane, where they interact with the plasma membrane-bound NOX2 and p22^{phox} subunits. Upon assembly of this complex, electrons are transferred from NADPH to oxygen to produce the superoxide anion and consequently other ROS. One limiting step in the assembly of this active NADPH oxidase complex is the binding of p67^{phox} to the activated, GTP-bound Rac1 and/or Rac2 (Abo et al., 1991; Diekmann et al., 1994; Lapouge et al., 2000). To this end, upon stimulation, cytosolic Rac1/2-GDP is released from the GDP dissociation inhibitor (Lambeth, 2004), allowing guanine nucleotide exchange factors (GEFs) to bind to Rac-GDP and catalyze the exchange of GDP for GTP (Etienne-Manneville and Hall, 2002). Once activated, Rac1/2-GTP translocate to the plasma membrane and recruits p67^{phox} by binding to its N-terminus (Koga et al., 1999; Lapouge et al., 2000). The binding of p67^{phox} to Rac1/2-GTP allows for the complete assembly of the complex and activation of NOX2 NADPH oxidase. High-resolution X-ray crystal

structures along with mutant data have revealed that the Arg 38 and Arg 102 residues of $p67^{phox}$ create a deep binding pocket that is necessary for interaction with Rac1/2-GTP (Koga et al., 1999; Lapouge et al., 2000).

Rac1/2 GTPases of the Rho family of small GTPases are pleiotropic regulators of a multitude of downstream cellular processes (Etienne-Manneville and Hall, 2002). In response to extracellular signals, the interconversion of Rac-GDP and Rac-GTP occurs via interaction with GEFs and GTPase-activating proteins (GAPs) (Bosco et al., 2009; Etienne-Manneville and Hall, 2002; Van Aelst and D'Souza-Schorey, 1997). The outcome of Rac activities hinges on their ability to interact with specific effectors, which regulate cell growth or survival programs, actin dynamics, or ROS production machinery. Since upregulated expression or activity, rarely mutation, of Rac GTPases, is often associated with human pathologies, recent studies have shown that targeting Rac activation by GEFs may serve as a tractable therapeutic option in various pathological settings (Bosco et al., 2010; Gao et al., 2004; Müller et al., 2008; Thomas et al., 2007). Previous rational design and drug discovery approaches utilizing structural information to predict high-affinity binding small molecules that dock to a specific region of Rac1 involved in GEF interaction have yielded successful results in identifying inhibitory molecules in the Rac signaling axis (Gao et al., 2004; Nassar et al., 2006). However, given the multifacet role of the Rac1/2 GTPases, it can be expected that strategies targeting Rac effectors may be more beneficial in reducing undesired effects at the level of Rac signaling, as higher specificity may be achieved downstream from Rac.

To specifically inhibit the effector function of Rac1 in the NOX2 NADPH oxidase signaling axis, we have performed an in silico screen to identify inhibitors of the Rac1-$p67^{phox}$ interaction. This unprecedented approach of targeting a small GTPase effector may afford greater specificity and circumvent the blockade of multiple Rac-mediated functions, such as actin reorganization by Rac activity inhibitors like NSC23766 (Gao et al., 2004) or Compound 4 (Ferri et al., 2009). We found that small molecules that bind to the Rac1 binding pocket of $p67^{phox}$ can readily inhibit Rac1 interaction and abrogate ROS production with a high degree of specificity. This targeting strategy has generated a class of lead inhibitors of a pathologically relevant inflammatory pathway of Rac signaling with a defined structure-activity relationship.

RESULTS

Virtual Screening for Compounds Targeting the Rac1 Binding Site of $p67^{phox}$

The three-dimensional structure of $p67^{phox}$ in complex with Rac1 (Protein Data Bank [pdb] 1E96) was visually analyzed using PyMOL in order to determine the contact region between the two proteins. Extraneous objects, such as water molecules and ions, that did not belong to the protein complex were removed. The structure of the Rac1-$p67^{phox}$ complex is shown in Figure 1A, where Arginine residues 38 and 102 of $p67^{phox}$ surround the site within the Rac1 interaction interface, and Rac1 residues 25–27 (Thr-Ans-Ala motif in Switch I) are buried upon complex formation and are sandwiched by Arg38 and Arg102. Next, the Rac1 chain was then displaced from the complex and the molecular surface representation of $p67^{phox}$ residues involved in the interaction with Rac1 was visually inspected to identify suitable small-molecule binding sites. A concave surface comprising Arg 102 and Arg 38 was qualitatively selected as the binding site for virtual screening (Koga et al., 1999; Lapouge et al., 2000). This crystallographic structure of $p67^{phox}$ was subsequently overlapped and aligned with the N-terminal region of another $p67^{phox}$ structure (pdb 1HH8) crystallized not in complex with Rac1. Negligible differences were observed from the root mean square deviation (RMSD) analysis in the spatial region involved in the Rac1-$p67^{phox}$ interaction, suggesting the conformation of the chosen docking pocket is mostly conserved before and after Rac1 binding and is suitable for virtual screening.

Virtual screening was performed using Autodock 4 for docking calculations of 350,000 diverse drug-like compounds from the proprietary University of Cincinnati Drug Discovery Center (UCDDC) compound library and from the public ZINC library, which contains over 700,000 compounds (Irwin and Shoichet, 2005; Morris et al., 2009). Automated docking was performed according to the docking flowchart (Figure 1B). The Autodock 4-conformed UCDDC and ZINC libraries were screened using the Lamarckian genetic algorithm (LGA) in three successive steps (Figure 1C). During the first two steps, the docking results were ranked for the lowest binding energy change, and the two sublibraries containing the selected hits were populated using a $DG_{binding}$ cut-off of −6.7 and −8.0 kcal/mol, respectively, for subsequent docking steps. The top hits derived were visually inspected using the AutoDockTool (ADT) by considering several parameters, such as $DG_{binding}$, cluster convergence, hydrogen bonding, and predicted molecular geometry. The selected top 100 hits were ranked for predicted water solubility (LogS), and compounds with $LogS < -4.3$ were chosen for further evaluation.

The chemical structure of one of the top hits, Phox-I1, in complex with $p67^{phox}$ is shown in Figure 1D. Hydrogen donor/acceptor interactions occur between the two nitro groups of the inhibitor and the Arg 102 and Arg 38 on $p67^{phox}$. The predicted binding energy ($DG_{binding}$) was −8.90 Kcal/mol, which is equivalent to a Ki of 2.9×10^{-7} M^{-1}. Further, Lipinski parameters and Ki's were calculated for the top nine predicted candidates specific for $p67^{phox}$ (Figure 1E).

Phox-I1 Binds to $p67^{phox}$ Target

To test the ability of the lead compounds identified by virtual screening to bind to the $p67^{phox}$ protein in the N-terminal 200 amino acid region necessary for Rac1-GTP interaction (Ahmed et al., 1998; Diekmann et al., 1994; Han et al., 1998), we employed microscale thermophoresis (Wienken et al., 2010). This technology probes for fluorescent changes in the hydration shell of molecules in order to measure protein-protein or protein-small molecule interactions with high sensitivity in near-native conditions. The $p67^{phox}$ N-terminus showed binding activity to the Phox-I1 compound in titration assays, yielding a Kd value of ~100nM (Figure 2A). Mutagenesis of R38 residue of $p67^{phox}$, which is critical for Rac1-GTP binding, disrupted the binding ability of Phox-I1 to $p67^{phox}$ (Figure 2B). As a positive control, a mutant made at residue R188 of $p67^{phox}$, outside of the region critical for interaction with Rac1-GTP (Koga et al., 1999; Lapouge et al., 2000), retained the binding activity to Phox-I1 (Figure 2C).

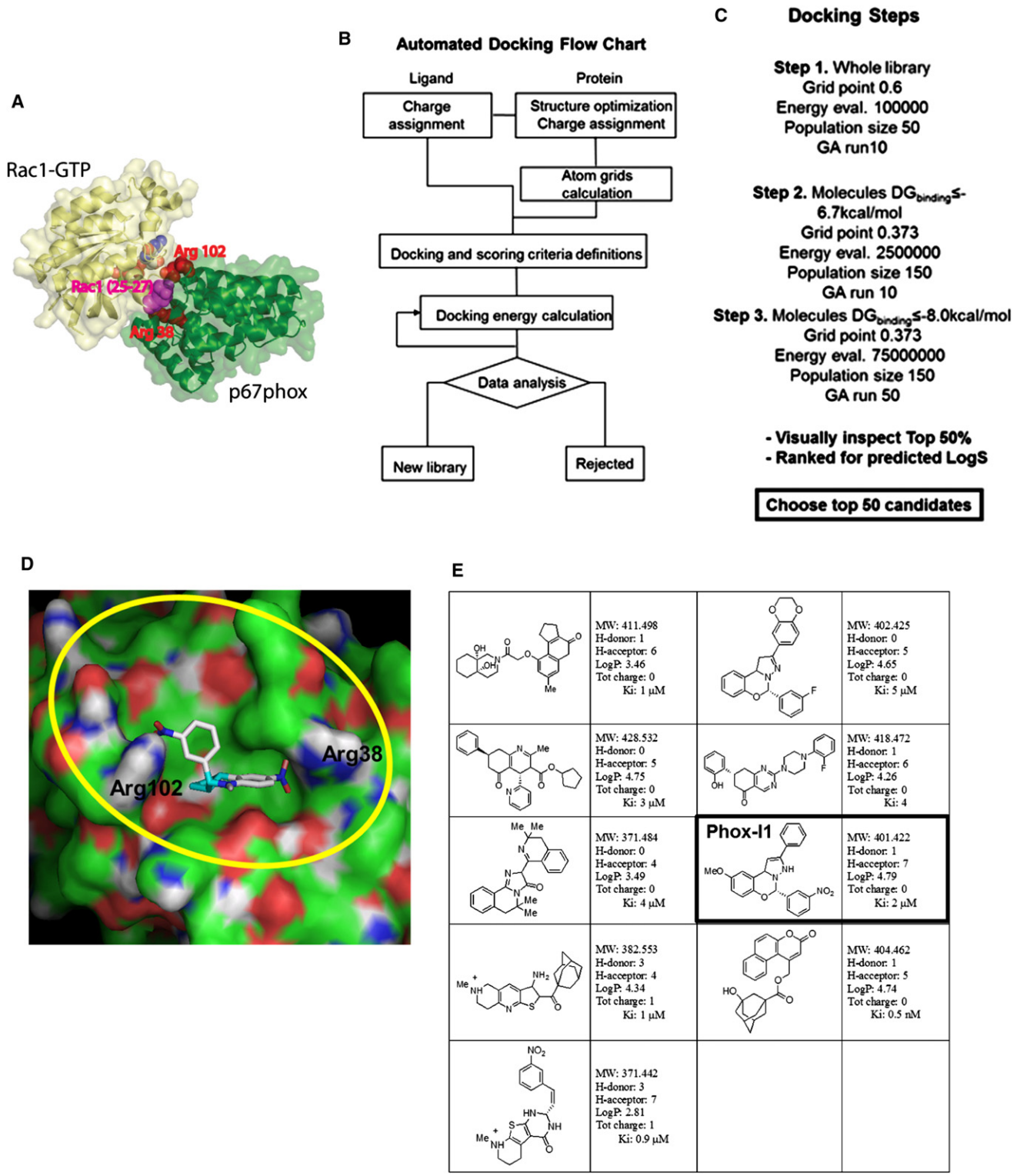

Figure 1. Virtual Screening of p67^{phox} Inhibitors from the ZINC and UC DDC Small Molecule Libraries

(A) The structure of the Rac1-p67^{phox} complex is shown. Rac1 is shown in yellow, whereas p67^{phox} is shown in green, respectively. Arginine residues 38 and 102 of p67^{phox}, which surround the site within the interaction interface that was targeted by virtual screening, are shown using red spheres. Rac1 residues 25–27 (Thr-Ans-Ala motif in Switch I), which are buried upon complex formation and are sandwiched by Arg38 and Arg102, are shown in magenta. Arg38 is directly involved in interface formation.

(B) The flowchart reports the strategy that was implemented for automated docking. Autodock 4 and related scripts were utilized to assign charges and perform docking energy calculations.

To demonstrate the ability of Phox-I1 to compete with active Rac1 for the binding pocket of $p67^{phox}$, we first validated the high-affinity binding activity of the constitutively active Rac1V12 mutant with $p67^{phox}$ by microscale thermophoresis (Figure 2D). Rac1-GDP was unable to bind to $p67^{phox}$ in this assay and thus showed specificity of this interaction for the active Rac1 (Figure 2E). Next, to perform a competition binding, $p67^{phox}$ protein was first incubated with either 5 μM Phox-I1 or an equal volume of vehicle control for 15 min prior to titration of purified Rac1V12 protein. The disruption of $p67^{phox}$ binding to Rac1V12 by Phox-I1, but not vehicle control, was evident (Figure 2F). Furthermore, as a control for specificity, Rac1V12 protein was incubated with various concentrations of Phox-I1, but no detectable binding was observed (Figure 2G). Thus, Phox-I1 binding to $p67^{phox}$ is specific and not due to nonspecific effects, such as aggregation (McGovern et al., 2002). Together, these studies indicate that the lead $p67^{phox}$ inhibitor Phox-I1 can bind to the Rac1 interactive site of $p67^{phox}$ specifically and interfere with Rac1-GTP interaction with $p67^{phox}$.

Phox-I1 Is Active in Suppressing ROS Production in Neutrophils

To validate the hits from virtual screening in cells, we performed several cellular functional assays using different cell types to measure the effect of compounds on inhibition of ROS production. ROS levels were first analyzed by fluorescence-activated cell sorting (FACS) in HL-60 pre-incubated with compounds for 2 hr prior to stimulation of ROS production. Because inhibitors of ROS production and NADPH oxidase activity are well studied in vitro and have been tested in clinical applications, we tested the lead $p67^{phox}$ inhibitor, Phox-I1, against NAC (a ROS scavenger), DPI (a broad range inhibitor of NADPH oxidase), and NSC23766 (a Rac-GTP inhibitor; Figure 3A). Phox-I1, at 20 μM, was able to attenuate ROS production similarly to 100 μM DPI or 100 μM NSC23766 and slightly more efficiently than 5 mM NAC. H_2O_2 added to the cells was included as a positive control for ROS measurement. Second, to test the capacity of Phox-I1 to inhibit ROS production in a primary cell context, primary murine neutrophils isolated from mouse bone marrow were treated with increasing concentrations of Phox-I1 and the efficacy of inhibition of fMLP-stimulated ROS production was analyzed. DPI treatment was included as a positive control for inhibition of ROS production (Figure 3B). Both 10 μM and 20 μM concentrations of Phox-I1 were able to inhibit ROS production nearly as well as DPI at 100 μM concentration. Next, to ascertain the optimal effective dose for ROS inhibition in cells, a dose titration series of Phox-I1 was administered to dHL-60 cells (Figure 3C). Optimal cellular response to this compound was achieved at doses of 10 μM with an IC_{50} of ~3 μM.

In addition to using the 2′-7′-dichlorodihydrofluorescein diacetate (DCFDA)-based FACS analysis of ROS generation in primary murine neutrophils, we validated the efficacy of Phox-I1 in primary human neutrophils by the luminol chemiluminescence assay. As shown in Figure 3D, Phox-I1 was able to suppress fMLP-induced ROS production in human neutrophils dose-dependently, with an IC_{50} ~8 μM, based on a one-site competition model. Further, Phox-I1 did not affect the exogenous glucose oxidase-produced ROS (Figure 3E) or the PMA-induced ROS production that is mediated through a PIP3-independent pathway (Figure 3F), suggesting that the fMLP-Rac-$p67^{phox}$ axis may mediate a pathway for NOX2 activation independently from the PMA pathway, consistent with previous studies indicating that fMLP and PMA induce superoxide generation through distinct pathways (Dong et al., 2005; Perisic et al., 2004). All together, these data indicate that Phox-I1 can efficiently inhibit ROS production in the μM range in both human and murine neutrophils.

Structure-Activity Relationship Analysis of Phox-I1 Structural Analogs

As discussed previously, the virtual screen led to the identification of Phox-I1 as a lead inhibitor of $p67^{phox}$. While this compound showed promising activity, progression to more advanced testing is limited by the generally poor solubility of the compound and toxicological concerns from the presence of nitro groups in the structure, as nitro groups are often associated with toxicity in animal studies and are rarely seen in clinical candidates. To develop a preliminary understanding of the structure-activity relationships (SAR) in these classes, we conducted a substructure search of the University of Cincinnati Drug Discovery Core chemical library. Thirty-five compounds from this search were visually screened in an attempt to explore the structural space with the goals of (1) retaining or improving activity, (2) improving solubility, and/or (3) seeking a replacement of the nitro groups. Toward that end, 16 compounds bearing more polar functional groups and with replacement or altered positions of the nitro groups were selected for further screening (Figure 4A).

To validate the relative potency of the compounds identified in the analog screen, we performed a cellular functional assay of ROS inhibition in differentiated HL-60 cells. Cells were pre-incubated with analogs from Figure 4A for 2 hr prior to stimulation of ROS production and analysis of ROS levels by FACS (Figure 4B). Comparing with cells treated with vehicle control, analogs 4, 10, 16, and Phox-I1 displayed the greatest inhibition of ROS production, whereas analogs 1, 7, 11, 12, and 13 showed little or no inhibition of ROS production. It is noteworthy that the structures of analogs 4 and 16, both of which displayed a high ROS inhibitory activity, are similar with the exception of one substituent, providing evidence of a core structure that is necessary for potency. Based on the improved ROS inhibitory activity displayed by analog 16, we termed it a second-generation lead inhibitor, Phox-I2. Although Phox-I2 serves as an attractive lead based on its improved ligand efficiency (maximum potency relative to size), it suffers from the presence of two nitro functions. Future plans are to further modify the structure and

(C) The main docking parameters adopted in the three different phases of the screening are displayed. The molecular geometry, cluster convergence, hydrogen bonding, and lowest predicted docking energy criteria have been used to select the best 50% of candidates coming from the third screening step.
(D) Molecular surface representation of $p67^{phox}$ in complex with a predicted inhibitor is displayed. The region comprising $p67^{phox}$ Arginine 102 and 38 is defined by our grids and is highlighted in yellow. Docked Energy: −8.77 Kcal/mol; Binding energy: −8.90 Kcal/mol, Ki 2.9×10^{-7} M^{-1}.
(E) A summary of the candidate inhibitors specific for $p67^{phox}$; parts of their Lipinski parameters and predicted Ki are reported on the side of each molecule.

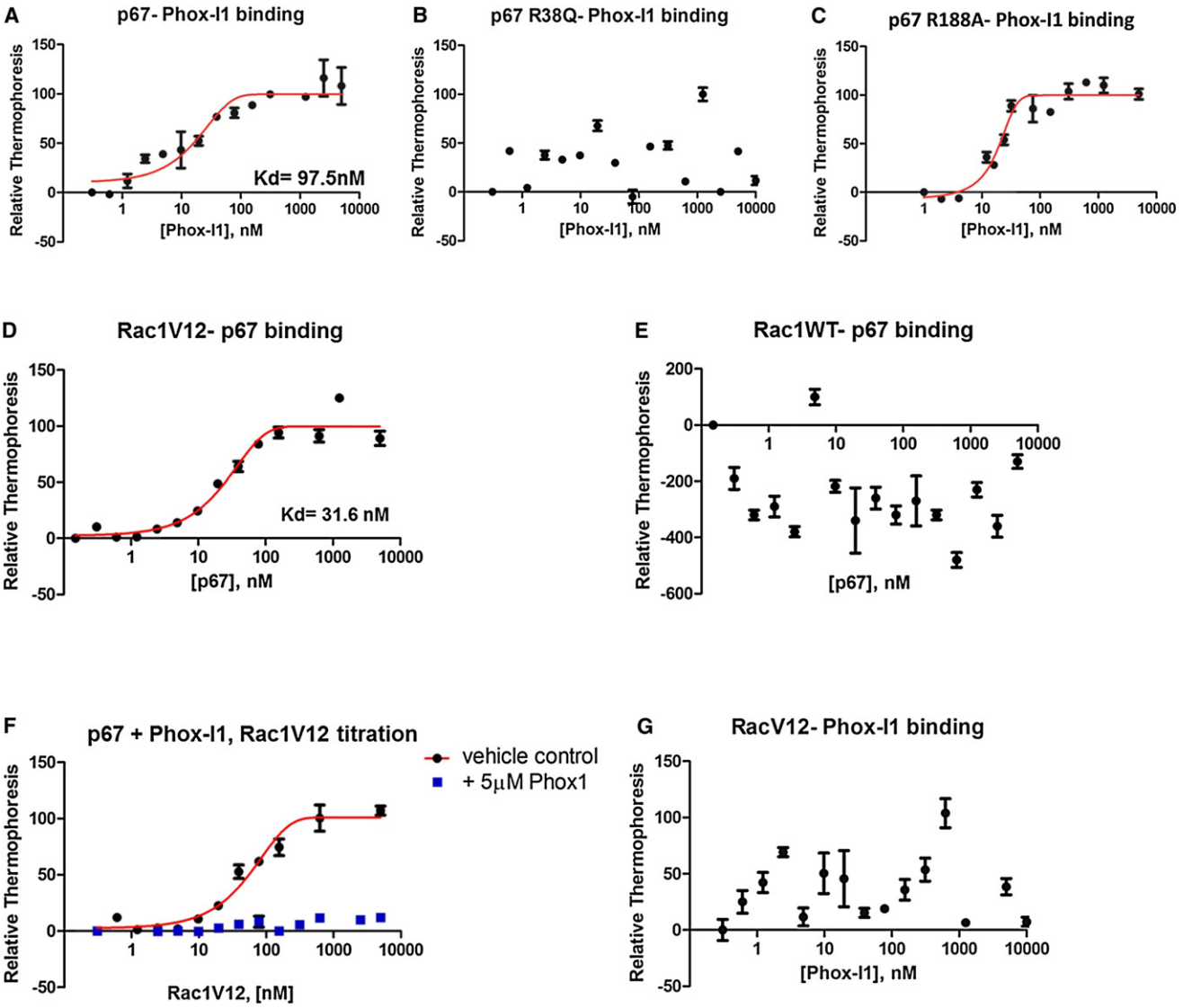

Figure 2. Binding Affinity and Specificity of Phox-I1 to p67^{phox}

(A) Using microscale thermophoresis, p67^{phox} recombinant protein (1-200) was able to bind Phox-I1 with a Kd of ~100 nM.

(B) Similar to (A), the ability of Phox-I1 to bind a recombinant mutant of p67^{phox} at the site critical for Rac1-GTP binding, p67R38Q, was tested by microscale thermophoresis.

(C) Experiment described in (B) was repeated with a random p67^{phox} mutation, R188A.

(D) Constitutively active Rac1V12 mutant protein binds p67^{phox} with a Kd of ~31 nM using microscale thermophoresis.

(E) However, Rac1 wild-type protein (predominantly in GDP- bound state) cannot bind p67^{phox} using microscale thermophoresis.

(F) Competitive binding of p67^{phox} with Phox-I1 or vehicle control, followed by titration of RacV12 protein using above methods.

(G) Phox-I1 is unable to bind RacV12 recombinant protein via above technique.

Error bars represent standard derivations.

adhere to standard guidelines of oral drug-like properties, such as the Veber and Lipinski rules (Lipinski et al., 2001; Veber et al., 2002).

To stringently confirm the effectiveness and specificity of these potential ROS inhibitors, it is advocated that multiple methods of measuring ROS production assays should be utilized (Jaquet et al., 2009). Therefore, to complement the DCFDA-based FACS analysis and the luminol chemiluminescence method, we performed nitroblue tetrazolium (NBT) assays in fMLP-activated primary murine neutrophils (Figure 4C). These experiments revealed that a 10 μM dose of Phox-I1 resulted in a significant blockade of superoxide production, which was heightened by similar treatment with Phox-I2. Both Phox-I1 and Phox-I2 were more effective at a lower dose than were our working concentration of DPI, which was included as a positive control for ROS inhibition. Thus, the results of these combined assay methods validated that the lead inhibitors could effectively inhibit ROS production by neutrophils.

We next confirmed the biochemical binding activity of Phox-I2 to p67^{phox} protein with a titration series of Phox-I2 using

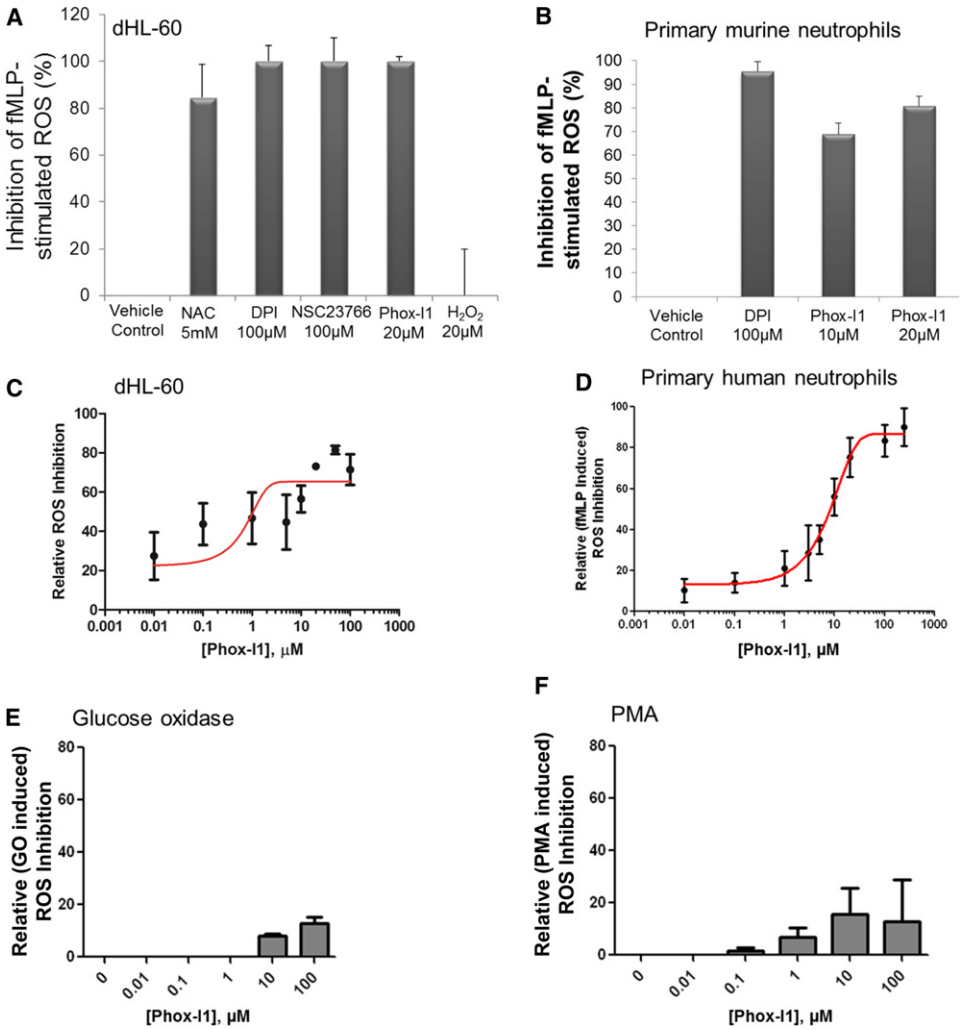

Figure 3. fMLP-Stimulated ROS Production Is Abrogated by Phox-I1 in Human HL-60 Cells and Primary Murine Neutrophils

(A) Ability of Phox-I1 to inhibit ROS production in fMLP-stimulated differentiated HL-60 cells as compared to standard ROS inhibitors was assessed by H2-DCFDA staining and FACS analysis. Levels of ROS production in non-fMLP-treated controls were subtracted from all samples; data was then normalized to fMLP-stimulated vehicle-treated control.

(B) Experiment described in (A) was repeated with primary murine neutrophils.

(C) As described in (A), HL-60 cells were treated with various concentrations of Phox-I1 and an IC_{50} curve was generated.

(D) Dose response of fMLP-induced ROS production to Phox-I1 by primary human neutrophils. Levels of ROS production in non-fMLP- or fMLP-stimulated human neutrophils were assayed by the luminol chemiluminescence method in increasing concentrations of Phox-I1. Data was normalized to fMLP-stimulated vehicle-treated control.

(E) Effect of Phox-I on glucose oxidase-generated ROS.

(F) Effect of Phox-I1 on PMA induced ROS production in human neutrophils assayed by the luminol chemiluminescence method.

Error bars represent standard derivations.

microscale thermophoresis (Figure 4D). As predicted based on in silico docking (data not shown) and core structural similarity to Phox-I1, Phox-I2 displayed a high-affinity binding to the $p67^{phox}$ target with an approximate Kd of ~150nM. Additionally, the dose-dependent potency of Phox-I2 was assessed in dHL-60 cells by the DCFDA assay, which revealed an IC_{50} ~1μM (Figure 4E), and in primary human neutrophils by the luminol chemiluminescence assay, yielding an IC_{50} ~6 μM (Figure 4F). As shown in Figure 3D, Phox-I1 was able to suppress fMLP-induced ROS production in human neutrophils dose-dependently. To validate our preliminary SAR information and as a negative control, analog 13 displayed no ROS inhibitory activity in dHL-60 cells (Figure 4B) and was unable to bind to $p67^{phox}$ protein (Figure 4G). Analog 13 was thereby unable to dose-dependently inhibit ROS production in the dHL-60 DCFDA ROS production assay (Figure 4H).

Specificity of Phox-I1 and Phox-I2 in Cells

Because several existing ROS inhibitors are associated with low potency and high cytotoxicity, we next assessed the levels of apoptosis in undifferentiated HL-60 cells treated with 20 or 100 μM Phox-I1, Phox-I2, or NSC23766 by FACS analysis for

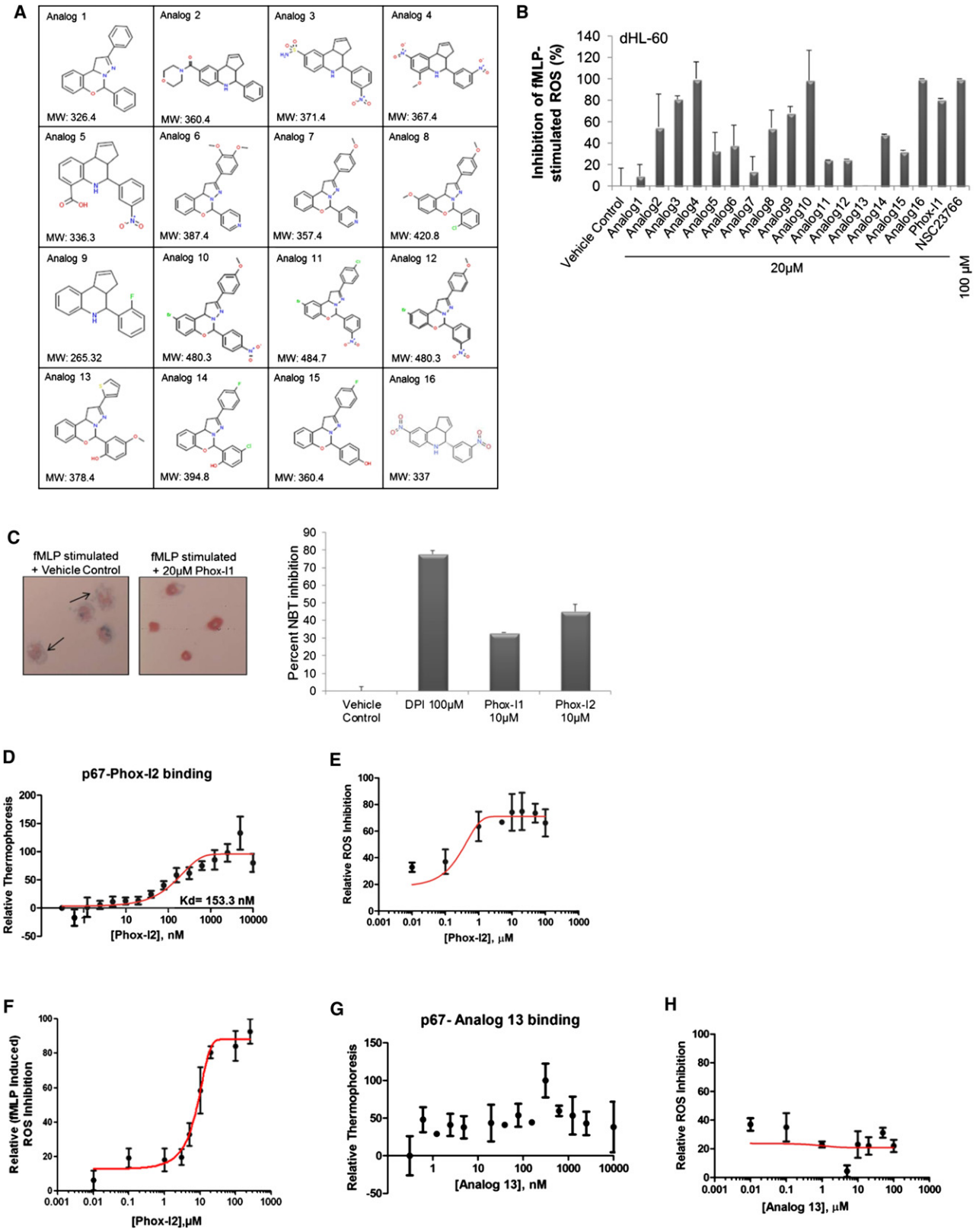

Figure 4. Phox-I1-Analog Analysis Yields Compounds with Improved or Similar Cellular ROS Inhibitory Activity

(A) List of analogs derived from a search of the UCDDC and ZINC compound libraries for Phox-I1-like structures with medicinal chemistry optimized features.
(B) H2-DCFDA staining in fMLP-stimulated dHL-60 cells treated with Phox-I1 analogs. Analogs 4, 10, and 16 (Phox-I2) all display improved ROS inhibition over Phox1.

Annexin V (Figure 5A). There was no detectable effect on cell apoptosis by NSC23766, Phox-I1, or Phox-I2 at either concentration as compared to the untreated control, indicating that these compounds have minimal cytotoxicity in the dosage range of maximal ROS inhibition. To analyze the biochemical specificity of these lead inhibitors on the effector pathways of active Rac1, undifferentiated HL-60 cells were treated with Phox-I1, Phox-I2, or NSC23766 for 18 hr. Immunoblot of the cell lysates was performed to probe the activity of a Rac effector other than $p67^{phox}$, Pak (Figure 5B). The phosphorylated Pak levels were abrogated by treatment with the Rac inhibitor NSC23766 but not Phox-I1 or Phox-I2, suggesting that Phox-I1 and Phox-I2 compounds are specific for the $p67^{phox}$ signaling arm of Rac-GTP, as opposed to Rac-GTP signaling in general, as is evidenced by NSC23766 treatment. Another method of addressing Rac-signaling specificity in neutrophils is by monitoring their ability to polarize actin to the leading edge upon fMLP stimulation. Importantly, neither Phox-I1, Phox-I2, nor an inactive analog 13 (all at 10 μM), were able to block the Rac-mediated dynamic process of F-actin polarization to the leading edge of primary murine neutrophils as observed by F-actin immunofluorescence imaging (Figure 5C, left panel). F-actin polarization was evident in about 80% of each treatment group of cells as in the control, untreated cells (Figure 5C, right panel). In contrast, Nocodazole (200 nM), a microtubule disrupting agent that was used as a positive control for disruption of the cytoskeleton, treated cells showed drastic reduction of polarized cells from 80% to ~20%. These data indicate that the Phox-I1 and Phox-I2 $p67^{phox}$ targeting agents do not affect Rac-mediated F-actin assembly. To test if the inhibitors are specific for the NOX2 enzyme, we carried out a xanthine/xanthine oxidase assay and found that Phox-I1 or Phox-I2 does not affect xanthine oxidase-mediated ROS production (Figure S2 available online). We further applied Phox-I1 to primary murine neutrophils expressing the constitutively active NOX4. As shown in Figure 5D, expression of NOX4 cDNA in neutrophils by nucleofection resulted in an elevated ROS production that is unresponsive to Phox-I1 treatment, in contrast to the fMLP-induced NOX2-mediated ROS response as assayed using a luminescence assay of L012 in the presence of HRP. To further rule out that Phox-I1 and Phox-I2 may simply act as scavengers of ROS, we pre-stimulated dHL-60 cells with fMLP for 30 min prior to treatment with Phox-I1 or Phox-I2. Unlike the ROS scavenger NAC, Phox-I1 and Phox-I2 do not affect the levels of superoxide that have already been produced, similarly to apocyanin, DPI, and NSC23766 (Figure 5E). Therefore, these lead $p67^{phox}$ inhibitors do not display antioxidant activity and are specific, consistent with their lack of inhibitory effect on glucose oxidase-induced ROS, as shown previously in Figure 3E.

The relevance of therapeutically targeting neutrophils in a pathological context is underscored by recent reports that the circulation time of human neutrophils in the periphery is longer than previously believed (<1 day versus 5.4 days; Pillay et al., 2010). We next performed a stability experiment to determine the duration of effectiveness of the compound in suppressing neutrophils. To analyze the relative affinities of these compounds for the $p67^{phox}$ target in cells, we performed DCFDA ROS production assays in dHL-60 cells treated with compound for 2 hr followed by wash and recovery for 4 hr or 2 hr in normal media prior to ROS production analysis. Although Phox-I1 ROS inhibitory activity was still evident 4 hr or 2 hr after washing the cells, Phox-I2 and analog 4 did not display effective ROS inhibition following removal of the compounds at the dosage tested (Figure 5F). In comparison, the tested dosages of NAC and NSC23766 both retained the ability to inhibit ROS production following a wash of the cells. To assess the relative stability of these compounds in culture over time, DCFDA ROS assays were performed in dHL-60 cells following the indicated time of exposure to the compound. None of the compounds were effective at inhibiting ROS production after 18 hr exposure in culture. Phox-I1 seemed to be the most stable in culture over time, displaying no significant change in efficacy in a 6 hr treatment window, whereas Phox-I2 and analog 4 retained some efficacies over 6 hr of treatment with more varied capacity to inhibit ROS (Figure 5G). Taken together, these data suggest that Phox-I1 and its derivatives display high biochemical and cellular activities in culture with a turnover time of >2–4 hr, indicating that their inhibitory effect is not short-lived, but a continuous supply is required for maximum effectiveness in overnight culture conditions.

Structure-Activity Relationship Analysis of Phox-I2

To further define the structure-activity relationship of Phox-I2, we performed medicinal chemistry synthesis of analogs of Phox-I2 to rationalize the key components of the structure for cellular activity. Compounds with similar structures to Phox-I2 through replacement of each nitro group, or addition of an extra aromatic ring to make the compound more "Phox-I1 like," were synthesized. Specifically, based on the Phox-I2 structure, seven compounds of four different categories, as shown in Figure 6A, were produced. When the ROS inhibitory activities of these compounds were tested by DCFDA FACS analysis in differentiated HL-60 cells, all compounds displayed activity (Figure 6B). It became evident that it is possible to replace the nitro group and retain activity (as shown by analog 22). This was further validated by the NBT assay in primary murine neutrophils where many of the analogs displayed partial activity, with analog 22 (fluorine groups replacing the outermost nitro groups) exhibiting

(C) Freshly isolated primary murine neutrophils were stimulated with fMLP to initiate ROS production; cells were then treated with DMSO control, DPI, Phox-I1, or Phox-I2 and a Nitroblue tetrazolium (NBT) assay was performed and imaged (left panel). Blue stain is superoxide anion; pink stain is neutrophil nucleus. Cells displaying ROS production were quantified from the images and non-fMLP treated ROS levels were subtracted prior to normalization to vehicle-control treated sample (right panel).
(D) Using microscale thermophoresis, $p67^{phox}$ protein binds to Phox-I2 with high affinity.
(E) IC_{50} for Phox-I2 was assayed by H2-DCFDA ROS production method in dHL-60 cells.
(F) Phox-I2 dosage response of ROS production in human neutrophils assayed by luminol chemiluminescence.
(G) As a negative control, analog 13 was unable to bind $p67^{phox}$.
(H) Anolag 13 showed no cellular ROS inhibitory activity in HL-60 cells.
Error bars represent standard derivations.

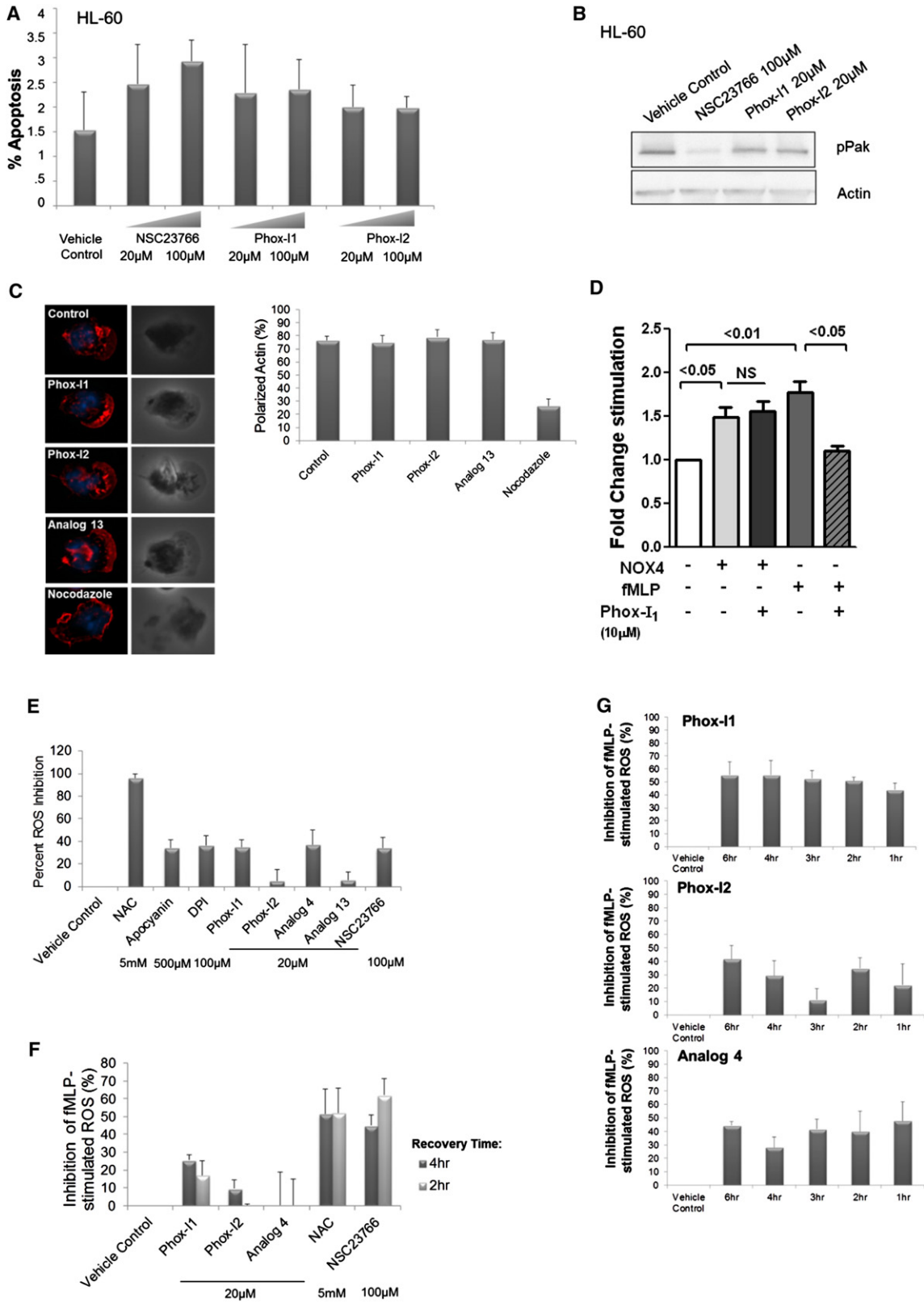

Figure 5. Phox-I1 and Phox-I2 Show Undetectable Toxicity and Site Effects

(A) Apoptosis analysis by FACS of HL-60 cells treated with compound or vehicle control for 2 hr prior to 7-AAD and Annexin V staining.

(B) HL-60 cells from (A) were harvested and lysates were immunoblotted for levels of pPAK, and actin was used as a control for loading.

profound superoxide inhibition (Figure 6C). These studies further define SAR of Phox-I2 structure and provide a solid ground for future optimization.

DISCUSSION

Because of the extensive role of NOX2 NADPH oxidase in innate immunity and pathophysiology, specific and effective inhibitors of this enzymatic complex have been long sought after but have proven to be challenging to develop. Several inhibitors of different components of the NADPH oxidase complex have previously been characterized, including apocyanin, diphenylene iodonium (DPI), gp91tat, NSC23766, and, most recently, VAS2870. Although these inhibitors have been useful in broadening our understanding of the role of the NADPH oxidases in disease, they may not be promising candidates for further drug development because of problems related to toxicity, potency, and specificity (Aldieri et al., 2008; Jaquet et al., 2009; Lambeth et al., 2008). Collectively, most studies using these inhibitors underscore the need for the development of a highly specific and nontoxic inhibitor of NOX2. Recent studies that utilize peptide inhibitors of the Rac1-GTP–NOX2 interaction, although potentially limited by drug delivery issues, have yielded significant inhibition of ROS production, further validated the targeting approach focusing on Rac interaction with this enzyme complex (Dahan et al., 2002; Morozov et al., 1998; Rey et al., 2001).

Here we have carried out a structure-based virtual screen to identify small molecules capable of specific interaction with the Rac1 binding pocket of $p67^{phox}$. This interaction by small molecule compounds abrogates the ability of active Rac1 binding to $p67^{phox}$ and subsequent activation of the NOX2 oxidase complex in murine and human neutrophils. The efficacy of these compounds is impressive given the potential contribution to ROS production by non-Rac dependent sources, such as NOX4, NOX5, and DUOX1/2, or mitochondrial ROS generation and reflects the strong dependency of NOX2 in neutrophils for ROS production. In fact, many NADPH oxidase related pathologies are mediated through the NOX2 enzyme, which requires Rac1/2 and $p67^{phox}$ binding for its activity (Bedard and Krause, 2007; Lambeth et al., 2008). As such, the $p67^{phox}$ inhibitor design described herein could serve as a principle for future development into clinically relevant leads. Additionally, this approach of targeting the $p67^{phox}$ constituent of the NADPH oxidase complex rather than Rac GTPase itself may circumvent a debate in the field regarding the Rac regulatory mechanism in NADPH oxidase complex activation (Bokoch and Diebold, 2002; Kao et al., 2008).

Prior work from our lab utilizing a similar rational design approach has yielded a specific inhibitor of Rac GTPases, NSC23766, which has been prolific, providing us with not only molecular mechanisms but also a preclinical therapeutic tool to build upon for translational applications (Gao et al., 2004; Nassar et al., 2006). However, in the case of NSC23766, all downstream effectors of Rac GTPases are inhibited due to a suppression of Rac activity, thereby causing potentially undesired effects resulting from inhibition of multiple effector pathways. The approach described here is, to our knowledge, the first time the small GTPase interactive site of an effector has been rationally targeted, setting up a proof of principle that it can be a viable tactic for enhancing the specificity of inhibitors in the context of small GTPase-mediated cellular functions. Further, in terms of lead discovery and development, the advantages of our small molecule approach to NADPH oxidase inhibition are several-fold. First, lead small molecules yielded from a rational design approach, rather than a high-throughput functional screen, are likely to display specificity and potency, which have been primary drawbacks of several NADPH oxidase inhibitors described previously. For example, DPI lacks specificity because it inhibits all NOX isoforms, nitric oxide synthase, xanthine oxidase, mitochondrial complex 1, and cytochrome P-450 reductase (Aldieri et al., 2008; Bedard and Krause, 2007); whereas apocyanin is thought to nonspecifically inhibit NOX through an indirect mechanism only at high dose (Lambeth et al., 2008; Lapperre et al., 1999; O'Donnell et al., 2003). Second, Phox-I1 and Phox-I2 inhibitors can suppress NADPH oxidase activity dose-dependently in a relative short time window, thereby reducing the risk of abolishing the phagocyte immune response. Third, peptide inhibitors, although specific and effective at inhibition of ROS production (Lambeth et al., 2008), may have limitations with oral drug delivery that can be overcome by modifications of small molecule inhibitors, such as those described here. Moreover, the rational design approach of virtual screening allows for the validation and optimization of "drug-like," soluble, and potent compounds that are more suitable for applications.

An advantage of small-molecule screening is the ability to optimize the potency of the compound through analysis of related analogs. The initial SAR profiles derived from these studies allow for future development of compounds with an improved potential for applications. With respect to Phox-I1 and Phox-I2, one of the initial blockades to application would be the presence of the nitro groups in both compounds, which

(C) F-actin reorganization in freshly isolated fMLP-stimulated primary murine neutrophils was analyzed. Representative images (left panel) and quantification (right panel) are displayed. Treatment with analog 13 is included as a "dead analog" that possesses no intrinsic ROS inhibitory activity, and nocodazole is included as a positive control for actin disruption. Cells were exposed to a 10 μM dose of Phox-I1, Phox-I2, and analog 13, as well as 200 nM nocodazole.
(D) The effect of Phox-I on NOX4-mediated ROS production was tested in primary murine neutrophils transfected with a NOX4 expressing plasmid. Phox-I1 at 10 uM Phox-I1 was applied to the cells for 30 min prior to ROS assay by luminol chemiluminescence in the presence of HRP. The fMLP-stimulated ROS activity in the presence or absence of 10 uM Phox-I1 was measured in parallel. See also Figure S2.
(E) The antioxidant abilities of these lead compounds were tested by prestimulating dHL-60 cells with fMLP for 30 min prior to treatment with Phox-I1 or Phox-I2. Levels of superoxide were analyzed by DCFDA assay and FACS. NAC-, apocyanin-, DPI-, and NSC23766-treated cells served as controls.
(F) For affinity assay, DMSO-differentiated HL-60 cells were treated with standard effective dose of indicated compound for 2 hr, washed, and allowed to recover in normal media for 4 hr or 2 hr prior to fMLP stimulation and DCFDA ROS production assay by FACS analysis.
(G) For stability assay, DMSO-differentiated HL-60 cells were treated with 20 μM dose of compound for the indicated time period prior to fMLP stimulation and DCFDA ROS production assay by FACS analysis. Thirty minutes and 18 hr time periods are not displayed because they revealed no ROS inhibition.
Error bars represent standard derivations.

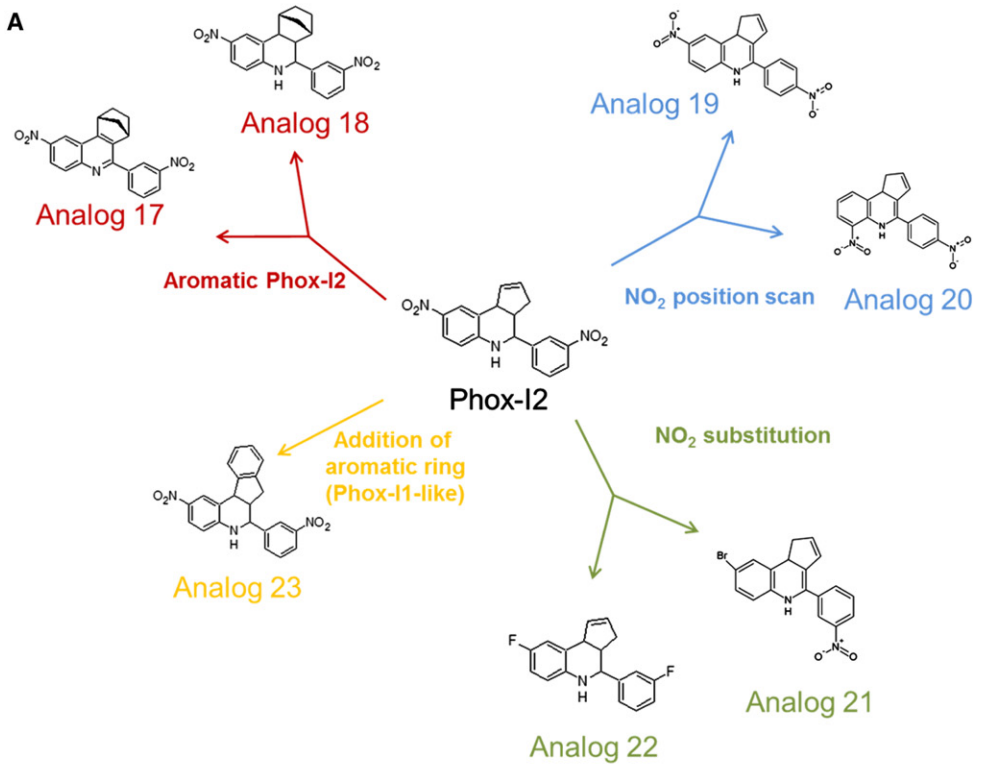

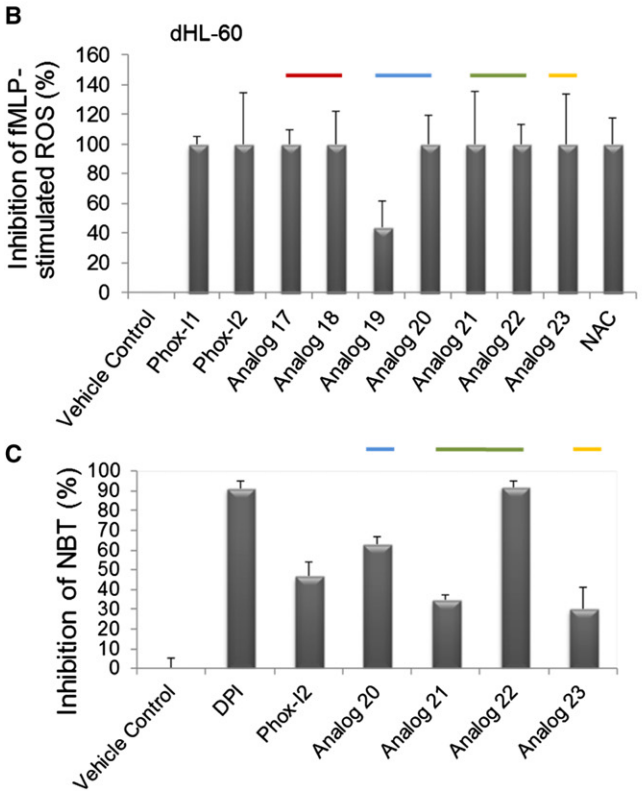

Figure 6. Medicinal Chemistry Optimization of Phox-I2 Allows for the Replacement of Potentially Toxic Nitro Groups

(A) Compounds with similar structures to Phox-I2 were synthesized and broken down into four different categories: (1) NO_2 position scan; (2) NO_2 substitution; (3) Addition of an aromatic ring (rendering it similar to Phox1); and (4) Aromatic Phox2.

(B) DCFDA FACS analysis was performed using differentiated HL-60 cells treated for 2 hr with compounds from A prior to stimulation with fMLP.

can be associated with toxicological concerns based on their ability to damage DNA following reductive activation. Thus, a major objective for the initial analog screening and secondary analog synthesis SAR studies was to understand the requirement of these groups in the compound structure. First, the analog screening experiments performed herein (Figure 4) allowed for the compounds to be grouped into two classes of structure, analogs 1, 6, 7, 8, 10, 11, 12, 14, and 15 were characterized as more Phox-I1-like, whereas analogs 2, 3, 4, 5, and 9 were defined as more Phox-I2-like. The SAR within the class of compounds derived from Phox1 was not well defined. Analog 1 revealed that the bare scaffold had little to no intrinsic activity. Analog 10 suggested that the addition of a substituent on the north phenyl ring was inconsequential, which is supported by the analog pairs of 11/12 and 8/14. This indicates that the north phenyl ring may be a region where substituents may be added to improve physical properties if a Phox-I1-like structure is to be pursued. In line with the key objective of reducing toxicity, analogs 6, 8, 14 and 15 demonstrated that some level of activity was retained in absence of nitro groups, albeit potency was significantly reduced. However, the set of analogs that are related to Phox-I2 show a clear SAR pattern in which specific changes resulted in specific effects on activity. Analog 4 indicated that a substituent at the 6 position could be added without severe activity consequences, although analog 5 suggested that this substituent should be less polar. Analogs 2 and 3 illustrated that the NO_2 group could be replaced with more hydrophilic functions without catastrophic loss of activity, which would be hopeful for improving the toxicological profile and solubility. Importantly, analog 9 demonstrated that the bare scaffold (no NO_2 groups) retains some intrinsic activity, thereby supporting the nonessentiality of the nitro functions. Nitro groups are particularly vexing since they have quite unique binding properties with no particularly effective bioisosteres. Analog 9 displayed similar potency to Analogs 2 and 5, suggesting the 3′ NO_2 may have less impact on activity. Thus, exploration of alternatives at this portion of the Phox-I2-like molecule subsequently became a major goal of the secondary synthetic screening effort described in Figure 6. One useful SAR conclusion from the compound synthesis experiments is that although deletion of the nitro groups altogether or shifting their position may negatively affect activity, nitro group substitution with fluorine maintains ROS inhibitory activity of the compound. Thus, removal of the potentially toxic nitro groups is possible and warrants further exploration and characterization.

Although structurally diverse, it is striking that the compounds identified by our rational design approach and subsequently the analogs derived from medicinal chemistry contain extended double-bond conjugated systems. These structures are described to be capable of mediating electron exchange as it would occur during ROS generation, and in this respect the $p67^{phox}$ inhibitors described here share similarities to some leading NOX inhibitors developed by the pharmaceutical industry (Jaquet et al., 2009).

In order to complement the in silico and cellular results, we also tested the Phox-I leads in cell-free superoxide production assays. Phox-I2 was able to dose-dependently inhibit Rac1-GMPPNP induced superoxide burst under the reconstitution conditions (Figure S3), consistent with the mode of action proposed for the inhibitor. However, the dose curve displayed a higher concentration shift of Phox-I2 than that required in the $p67^{phox}$ binding and cell assays. The requirements of higher concentration of inhibitors in the cell free assay have been previously observed for peptide-based NOX2 inhibitors (Joseph and Pick, 1995; Dahan et al., 2002). Further investigation is necessary to provide insight into this difference. Moreover, there is a difference in target p67 binding affinity (Kd) and ROS inhibitory efficacy in cells (IC_{50}) by the inhibitors, at close to 2 order of magnitude; this could be related to multiple factors such as the route/efficacy of entry, stability, metabolism, etc., in cells.

NAC, a global ROS scavenger, has been described to have a positive effect in a broad array of pathologies such as neurological disorders (Berk et al., 2008), cystic fibrosis (Tirouvanziam et al., 2006), and cancer progression (Estensen et al., 1999; Radisky et al., 2005; van Zandwijk et al., 2000), but its effect is broad and nonspecific. Although therapies directed at components of the NOX enzyme have shown promise in disorders including metabolic dysfunction of the pancreatic β-cell, neuronal degeneration following cerebral ischemia, therapeutic resistance in hematological malignancy, and cardiovascular disease (Bedard and Krause, 2007; Kleinschnitz et al., 2010; Kowluru, 2011; Raz et al., 2010; Sawada et al., 2010; Velaithan et al., 2011; Williams and Griendling, 2007), none of the existing NOX inhibitors are ready for application in the clinics due to issues of toxicity and efficacy. Therefore, drugs which potently and specifically inhibit ROS production by NOX enzymes are an unmet clinical need that will have far-reaching implications, and strategies for their development, such as the one described here, are critical. To this end, targeting of small GTPases has emerged as an attractive area of lead development (Nassar et al., 2006). However, effective inhibition of a signaling node of a small GTPase that controls a multitude of effector pathways, as seen with a Rac targeting agent such as NSC23766, could also yield increased toxicity and nonspecific effects. The current approach of targeting one specific effector of Rac could circumvent this concern. Importantly, not only may our rationally design approach has potential implications in diseases mediated by inflammatory responses, but it also presents an avenue for generating lead inhibitors of other effectors for pathologically relevant small GTPase signaling axes, including that of Ras, Rab, and Rho.

SIGNIFICANCE

Because of the wide array of cellular functions regulated by Rho GTPase activities and the numerous pathologies to which their deregulation may contribute, their signaling axes serve as attractive drug targets. Recently, a number of studies have utilized NSC23766, a Rac activation inhibitor,

(C) Freshly isolated primary murine neutrophils were stimulated with fMLP to initiate ROS production; cells were then treated with DMSO control, DPI, Phox-I2, and analogs 20, 21, 22, and 23. A nitroblue tetrazolium assay was performed and imaged in order to quantitate superoxide inhibition. Non-fMLP treated ROS levels were subtracted prior to normalization to vehicle control treated sample.
Error bars represent standard derivations.

to inhibit the activity and signaling events of Rac GTPases. However, this targeting approach blocks multiple downstream signaling pathways from Rac, and thus, may lack specificity for distinct cellular functions controlled by Rac. The current study aims to utilize structure-function information to rationally design inhibitors of a unique downstream effector of Rac GTPases. Upon Rac binding, the downstream effector, p67^{phox}, directly regulates the production of ROS by assembling the NOX2 NADPH oxidase complex. Since ROS generation via NADPH oxidase is implicated in a wide array of human diseases, it can be envisioned that specifically targeting the Rac1-p67^{phox} interaction will prevent activation of the oxidase and may serve as a tractable therapeutic option. As existing NADPH oxidase inhibitors lack specificity or potency, the development of novel inhibitors is important for evaluating the efficacy of NADPH oxidase targeting strategies. Here, we describe the rational design and characterization of small molecule inhibitors of the Rac-p67^{phox} interaction. The Phox-I1/Phox-I2 lead inhibitors bind p67^{phox} with submicromolar affinity and compete with the binding of activated Rac. Consequently, they are capable of abrogating superoxide production in neutrophils without affecting Rac-mediated actin cytoskeleton structure. Structure-activity relationship studies of the lead inhibitors have yielded promising analogs that are amenable to future optimization. Our studies present the first evidence, to our knowledge, that structure-function-based rational design can be a useful means of identifying inhibitors targeting the small GTPase-effector interface downstream of small GTPase signaling.

EXPERIMENTAL PROCEDURES

Virtual Screening

Virtual screening was performed to identify candidate molecules that could disrupt the formation of p67^{phox} complex with Rac1, by binding to p67^{phox} within the interaction interface with Rac1. Docking simulations for the virtual screening were performed using rigid body docking, as implemented in AutoDock (versions 3.5 and 4.0; Huey et al., 2007; Morris et al., 2009). A crystal structure of the complex (Lapouge et al., 2000; pdb 1E96) was used to build the model of the p67^{phox} receptor for the docking simulations, using ADT graphical interface to define the simulation grid boxes. Two libraries of compounds were used, including the drug-like subset of the ZINC library (Irwin and Shoichet, 2005) and in-house diversified library of about 340,000 drug-like compounds (assembled by the former Procter & Gamble Pharmaceuticals) now owned by the University of Cincinnati Drug Discovery Center (UCDDC). Gesteiger partial charges were used for both the receptor and ligands. Screening was performed in three stages using increasingly stringent parameters (e.g., changing grid density from 0.6 Ang in the initial screening to 0.375 in the refinement stage) and using gradually more extensive sampling by increasing the number of energy evaluations (from 100,000 to 10 mln), Genetic Algorithm runs (from 10 to 33), and population size (from 75 to 150). After initial fast screening, promising candidates with high estimated binding affinities were retained for the refinement stage. Candidate compounds were ranked based on their estimated binding affinities, and top candidates were further assessed from the point of view of their properties.

Protein Purification, Mutagenesis, and Microscale Thermophoresis

The p67^{phox} protein was expressed in BL21(DE3) bacteria (Stratagene, Santa Clara, CA, USA) using the pET30-HIS p67(1-212) plasmid. Protein was purified using the QIAexpress Ni-NTA kit (Qiagen, Valencia, CA, USA) or the GST Bind Resin Chromatography Kit (Novagen, Darmstadt, Germany) for RacV12 and RacWT proteins. Mutagenesis was carried out using the QuikChange Lightening Site-Directed Mutagenesis Kit (Stratagene). Proteins were labeled for microscale thermophoresis using the Monolith NT Protein Labeling Kit Red (NanoTemper Technologies, München, Germany), as recommended by the manufacturer. Binding reactions were carried out using the Monolith NT.115 (Nano Temper Technologies). Binding data was analyzed using Graphpad Prizm to estimate Kd values. The arbitrary fluorescence value from the thermophoresis plots for the smallest compound titration was subtracted from every other data point (Delta depletion) prior to normalization to a V_{max} of 100. In thermophoresis plots where there was no binding, a curve could not be fit, and therefore no V_{max} could be assigned. In these instances the highest delta depletion value was set to 100, and all data were normalized accordingly.

Cell Culture

HL-60 cells (a kind gift of Dr. Christopher Karp, Cincinnati Children's Hospital, Cincinnati, OH, USA) were propagated in RPMI 1640 medium containing 10% heat inactivated fetal bovine serum, 2 mM L-glutamine, and 100 U/ml penicillin/streptomycin at 37°C in air containing 5% CO_2. For differentiation, HL-60 cells were cultured in 1.3% dimethyl sulfoxide (DMSO) as previously described (Servant et al., 1999) to produce dHL-60 cells. Primary murine neutrophils were isolated from C57Bl/6 mouse bone marrow in accordance with a published protocol (Filippi et al., 2007) using a discontinuous Percoll (Pharmacia, New York, USA) gradient and were utilized immediately in experiments. Human neutrophils were obtained from fresh blood (IRB #2010-1855, Cincinnati Children's Hospital Medical Center) following a well-established protocol using density gradient separation from whole blood (Oh et al., 2008).

Chemicals and Synthesis

PMA, apocynin, H2O2, DPI chloride, DTT, HRP, glucose oxidase, xanthine, and xanthine oxidase were purchased from Sigma-Aldrich (St. Louis, MO, USA). All Phox-I compounds and derivatives, except for those used in initial screening, were custom synthesized by Radikal Therapeutics Inc. (Beverly, MA, USA). The chemicals were subjected to LC/MS analysis prior to use, as shown in an example in Figure S1.

Immunoblot Analysis

Whole-cell lysates were prepared by cell extraction using lysis buffer containing 20 mM Tris-HCl (pH 7.6), 100 mM NaCl, 10 mM $MgCl_2$, 1% Triton X-100, 0.2% sodium deoxycholate, 1 mM phenylmethylsulfonyl fluoride, 10 μg/ml of leupeptin, 1 μg/ml of aprotinin, and 1 mM dithiothreitol for 30 min. Equal amounts of protein, as determined by Bradford assay, were resolved by sodium dodecyl sulfate polyacrylamide gel electrophoresis. Specific proteins were detected by standard immunoblotting procedures using the following primary antibodies: (Cell Signaling, Danvers, MA, USA; 1:500 dilution) phospho-PAK1 (Ser144)/PAK2 (Ser141), (Sigma-Aldrich; 1:500) β-actin.

Flow Cytometry

Cells (5×10^5) were harvested and processed for Annexin V/ 7AAD staining in accordance with manufacturer's protocol (Becton Dickinson, Franklin Lakes, NJ, USA). Flow cytometry data were acquired on a FACS Canto bench-top flow cytometer (Becton Dickinson), and the cell cycle distributions were determined by a BrdU incorporation assay using Flo-Jo software (Bosco et al., 2010). For ROS production assay, primary murine neutrophils or dHL60 cells were incubated with compound for 2 hr prior to addition of H_2-DCFDA in accordance with the manufacturer's instructions (Molecular Probes, Grand Island, NY, USA). Cells were then stimulated with 10 μM fMLP (Sigma-Aldrich), 1mM $CaCl_2$, and 1.5 mM $MgCl_2$ for 15 min prior to wash and FACS analysis for mean fluorescence intensity. Non-fMLP stimulated control values were subtracted from all samples before normalization to fMLP-stimulated, vehicle control-treated sample in order to display percent ROS inhibition.

F-actin Immunofluorescence

Cells were pretreated with compound for 40 min prior to wash and resuspended in HBSS with compound. Cells were allowed to adhere to fibronectin (Sigma-Aldrich) coated glass coverslips (15 min) and then stimulated with 100 nM fMLP (3 min). Coverslips were then fixed with 3.7% paraformaldehyde (Sigma-Aldrich), and then staining for F-actin was performed with rhodamine phalloidin per the manufacturer's instructions (Molecular Probes).

Nitroblue Tetrazolium Assay

Primary neutrophils from mouse bone marrow were subjected to fMLP stimulation in the presence or absence of various chemicals for 5 min. Cells were stained for NBT activity as previously described (Filippi et al., 2004) to reveal relative ROS production.

Luminol Chemiluminescence Assay

Human neutrophils (2×10^5) were stimulated in HBSS supplemented with 0.1% BSA, 1mM Ca^{2+}, 1mM Mg^{2+}, and with fMLP (10 μM), PMA (300 nM) or glucose oxidase (200 mU/ml) for 30 min in the presence of 10 μM [8-amino-5-chloro-7-phenylpyrido[3,4-d]pyridazine-1,4(2H,3H)dione] L012. Chemiluminescence was measured using GloMax-96 Microplate Luminometer (Promega; Tarpey et al., 2004). The generation of hydrogen peroxide by the xanthine/xanthine oxidase was performed in phosphate buffered saline supplemented with xanthine oxidase (0.004 U), HRP (0.005 $U \cdot mL^{-1}$), and L012 (Wind et al., 2010). The reaction was started by the addition of xanthine (0.5 mM).

Amaxa Transfection of Primary Neutrophils

Primary mouse neutrophils were suspended in 100 μl Nucleofector solution with 10 μg plasmid pCDNA3-NOX4 encoding NOX4 (a kind gift of Dr. T. Leto, National Institutes of Health, Bethesda, MD, USA) or mock vector. Cells were transfected using a Cell Line V Nucleofactor kit (Amaxa Biosystem, Amaxa Inc., Cologne, Germany) and the Nucleofector program Y-001. Cells were recovered at 37°C for 2 hr and subjected to the luminol chemiluminescence assay using 10 μM L012 and HRP (0.005 $U \cdot ml^{-1}$) to record ROS produced by NOX4 expression.

SUPPLEMENTAL INFORMATION

Supplemental Information includes three figures and can be found with this article online at doi:10.1016/j.chembiol.2011.12.017.

ACKNOWLEDGMENTS

The authors thank all members of the Zheng lab for thought-provoking discussion and acknowledge the Cincinnati Children's Hospital Medical Center (CCHMC) Biomedical Informatics computational cluster and CCHMC institutional support for assistance in the virtual screening process. The work is partly supported by National Institutes of Health grants (R41 HL099244, R01 CA141341, and T32 HL091805). The authors have no conflict of interest to declare.

Received: July 20, 2011
Revised: December 8, 2011
Accepted: December 22, 2011
Published: February 23, 2012

REFERENCES

Abo, A., Pick, E., Hall, A., Totty, N., Teahan, C.G., and Segal, A.W. (1991). Activation of the NADPH oxidase involves the small GTP-binding protein p21rac1. Nature *353*, 668–670.

Ahmed, S., Prigmore, E., Govind, S., Veryard, C., Kozma, R., Wientjes, F.B., Segal, A.W., and Lim, L. (1998). Cryptic Rac-binding and p21(Cdc42Hs/Rac)-activated kinase phosphorylation sites of NADPH oxidase component p67(phox). J. Biol. Chem. *273*, 15693–15701.

Aldieri, E., Riganti, C., Polimeni, M., Gazzano, E., Lussiana, C., Campia, I., and Ghigo, D. (2008). Classical inhibitors of NOX NAD(P)H oxidases are not specific. Curr. Drug Metab. *9*, 686–696.

Armitage, M.E., Wingler, K., Schmidt, H.H., and La, M. (2009). Translating the oxidative stress hypothesis into the clinic: NOX versus NOS. J. Mol. Med. *87*, 1071–1076.

Bedard, K., and Krause, K.H. (2007). The NOX family of ROS-generating NADPH oxidases: physiology and pathophysiology. Physiol. Rev. *87*, 245–313.

Berk, M., Copolov, D.L., Dean, O., Lu, K., Jeavons, S., Schapkaitz, I., Anderson-Hunt, M., and Bush, A.I. (2008). N-acetyl cysteine for depressive symptoms in bipolar disorder—a double-blind randomized placebo-controlled trial. Biol. Psychiatry *64*, 468–475.

Bokoch, G.M., and Diebold, B.A. (2002). Current molecular models for NADPH oxidase regulation by Rac GTPase. Blood *100*, 2692–2696.

Bosco, E.E., Mulloy, J.C., and Zheng, Y. (2009). Rac1 GTPase: a "Rac" of all trades. Cell. Mol. Life Sci. *66*, 370–374.

Bosco, E.E., Ni, W., Wang, L., Guo, F., Johnson, J.F., and Zheng, Y. (2010). Rac1 targeting suppresses p53 deficiency-mediated lymphomagenesis. Blood *115*, 3320–3328.

Dahan, I., Issaeva, I., Gorzalczany, Y., Sigal, N., Hirshberg, M., and Pick, E. (2002). Mapping of functional domains in the p22(phox) subunit of flavocytochrome b(559) participating in the assembly of the NADPH oxidase complex by "peptide walking". J. Biol. Chem. *277*, 8421–8432.

Diekmann, D., Abo, A., Johnston, C., Segal, A.W., and Hall, A. (1994). Interaction of Rac with p67phox and regulation of phagocytic NADPH oxidase activity. Science *265*, 531–533.

Dong, X., Mo, Z., Bokoch, G., Guo, C., Li, Z., and Wu, D. (2005). P-Rex1 is a primary Rac2 guanine nucleotide exchange factor in mouse neutrophils. Curr. Biol. *15*, 1874–1879.

Estensen, R.D., Levy, M., Klopp, S.J., Galbraith, A.R., Mandel, J.S., Blomquist, J.A., and Wattenberg, L.W. (1999). N-acetylcysteine suppression of the proliferative index in the colon of patients with previous adenomatous colonic polyps. Cancer Lett. *147*, 109–114.

Etienne-Manneville, S., and Hall, A. (2002). Rho GTPases in cell biology. Nature *420*, 629–635.

Ferri, N., Corsini, A., Bottino, P., Clerici, F., and Contini, A. (2009). Virtual screening approach for the identification of new Rac1 inhibitors. J. Med. Chem. *52*, 4087–4090.

Filippi, M.D., Harris, C.E., Meller, J., Gu, Y., Zheng, Y., and Williams, D.A. (2004). Localization of Rac2 via the C terminus and aspartic acid 150 specifies superoxide generation, actin polarity and chemotaxis in neutrophils. Nat. Immunol. *5*, 744–751.

Filippi, M.D., Szczur, K., Harris, C.E., and Berclaz, P.Y. (2007). Rho GTPase Rac1 is critical for neutrophil migration into the lung. Blood *109*, 1257–1264.

Gao, Y., Dickerson, J.B., Guo, F., Zheng, J., and Zheng, Y. (2004). Rational design and characterization of a Rac GTPase-specific small molecule inhibitor. Proc. Natl. Acad. Sci. USA *101*, 7618–7623.

Han, C.H., Freeman, J.L., Lee, T., Motalebi, S.A., and Lambeth, J.D. (1998). Regulation of the neutrophil respiratory burst oxidase. Identification of an activation domain in p67(phox). J. Biol. Chem. *273*, 16663–16668.

Huey, R., Morris, G.M., Olson, A.J., and Goodsell, D.S. (2007). A semiempirical free energy force field with charge-based desolvation. J. Comput. Chem. *28*, 1145–1152.

Irwin, J.J., and Shoichet, B.K. (2005). ZINC—a free database of commercially available compounds for virtual screening. J. Chem. Inf. Model. *45*, 177–182.

Jaquet, V., Scapozza, L., Clark, R.A., Krause, K.H., and Lambeth, J.D. (2009). Small-molecule NOX inhibitors: ROS-generating NADPH oxidases as therapeutic targets. Antioxid. Redox Signal. *11*, 2535–2552.

Joseph, G., and Pick, E. (1995). "Peptide walking" is a novel method for mapping functional domains in proteins. Its application to the Rac1-dependent activation of NADPH oxidase. J. Biol. Chem. *270*, 29079–29082.

Kao, Y.Y., Gianni, D., Bohl, B., Taylor, R.M., and Bokoch, G.M. (2008). Identification of a conserved Rac-binding site on NADPH oxidases supports a direct GTPase regulatory mechanism. J. Biol. Chem. *283*, 12736–12746.

Kleinschnitz, C., Grund, H., Wingler, K., Armitage, M.E., Jones, E., Mittal, M., Barit, D., Schwarz, T., Geis, C., Kraft, P., et al. (2010). Post-stroke inhibition of induced NADPH oxidase type 4 prevents oxidative stress and neurodegeneration. PLoS Biol. *8*, 8.

Koga, H., Terasawa, H., Nunoi, H., Takeshige, K., Inagaki, F., and Sumimoto, H. (1999). Tetratricopeptide repeat (TPR) motifs of p67(phox) participate in interaction with the small GTPase Rac and activation of the phagocyte NADPH oxidase. J. Biol. Chem. *274*, 25051–25060.

Kowluru, A. (2011). Friendly, and not so friendly, roles of Rac1 in islet beta-cell function: lessons learnt from pharmacological and molecular biological approaches. Biochem. Pharmacol. *81*, 965–975.

Lambeth, J.D. (2004). NOX enzymes and the biology of reactive oxygen. Nat. Rev. Immunol. *4*, 181–189.

Lambeth, J.D., Krause, K.H., and Clark, R.A. (2008). NOX enzymes as novel targets for drug development. Semin. Immunopathol. *30*, 339–363.

Lapouge, K., Smith, S.J., Walker, P.A., Gamblin, S.J., Smerdon, S.J., and Rittinger, K. (2000). Structure of the TPR domain of p67phox in complex with Rac.GTP. Mol. Cell *6*, 899–907.

Lapperre, T.S., Jimenez, L.A., Antonicelli, F., Drost, E.M., Hiemstra, P.S., Stolk, J., MacNee, W., and Rahman, I. (1999). Apocynin increases glutathione synthesis and activates AP-1 in alveolar epithelial cells. FEBS Lett. *443*, 235–239.

Lipinski, C.A., Lombardo, F., Dominy, B.W., and Feeney, P.J. (2001). Experimental and computational approaches to estimate solubility and permeability in drug discovery and development settings. Adv. Drug Deliv. Rev. *46*, 3–26.

McGovern, S.L., Caselli, E., Grigorieff, N., and Shoichet, B.K. (2002). A common mechanism underlying promiscuous inhibitors from virtual and high-throughput screening. J. Med. Chem. *45*, 1712–1722.

Morozov, I., Lotan, O., Joseph, G., Gorzalczany, Y., and Pick, E. (1998). Mapping of functional domains in p47(phox) involved in the activation of NADPH oxidase by "peptide walking". J. Biol. Chem. *273*, 15435–15444.

Morris, G.M., Huey, R., Lindstrom, W., Sanner, M.F., Belew, R.K., Goodsell, D.S., and Olson, A.J. (2009). AutoDock4 and AutoDockTools4: Automated docking with selective receptor flexibility. J. Comput. Chem. *30*, 2785–2791.

Müller, L.U., Schore, R.J., Zheng, Y., Thomas, E.K., Kim, M.O., Cancelas, J.A., Gu, Y., and Williams, D.A. (2008). Rac guanosine triphosphatases represent a potential target in AML. Leukemia *22*, 1803–1806.

Nassar, N., Cancelas, J., Zheng, J., Williams, D.A., and Zheng, Y. (2006). Structure-function based design of small molecule inhibitors targeting Rho family GTPases. Curr. Top. Med. Chem. *6*, 1109–1116.

O'Donnell, R.W., Johnson, D.K., Ziegler, L.M., DiMattina, A.J., Stone, R.I., and Holland, J.A. (2003). Endothelial NADPH oxidase: mechanism of activation by low-density lipoprotein. Endothelium *10*, 291–297.

Oh, H., Siano, B., and Diamond, S. (2008). Neutrophil isolation protocol. J. Vis Exp. *17*, e745, 3791/745.

Perisic, O., Wilson, M.I., Karathanassis, D., Bravo, J., Pacold, M.E., Ellson, C.D., Hawkins, P.T., Stephens, L., and Williams, R.L. (2004). The role of phosphoinositides and phosphorylation in regulation of NADPH oxidase. Adv. Enzyme Regul. *44*, 279–298.

Pillay, J., den Braber, I., Vrisekoop, N., Kwast, L.M., de Boer, R.J., Borghans, J.A., Tesselaar, K., and Koenderman, L. (2010). In vivo labeling with 2H2O reveals a human neutrophil lifespan of 5.4 days. Blood *116*, 625–627.

Radisky, D.C., Levy, D.D., Littlepage, L.E., Liu, H., Nelson, C.M., Fata, J.E., Leake, D., Godden, E.L., Albertson, D.G., Nieto, M.A., et al. (2005). Rac1b and reactive oxygen species mediate MMP-3-induced EMT and genomic instability. Nature *436*, 123–127.

Raz, L., Zhang, Q.G., Zhou, C.F., Han, D., Gulati, P., Yang, L.C., Yang, F., Wang, R.M., and Brann, D.W. (2010). Role of Rac1 GTPase in NADPH oxidase activation and cognitive impairment following cerebral ischemia in the rat. PLoS ONE *5*, e12606.

Rey, F.E., Cifuentes, M.E., Kiarash, A., Quinn, M.T., and Pagano, P.J. (2001). Novel competitive inhibitor of NAD(P)H oxidase assembly attenuates vascular O(2)(-) and systolic blood pressure in mice. Circ. Res. *89*, 408–414.

Roos, D. (1994). The genetic basis of chronic granulomatous disease. Immunol. Rev. *138*, 121–157.

Sawada, N., Li, Y., and Liao, J.K. (2010). Novel aspects of the roles of Rac1 GTPase in the cardiovascular system. Curr. Opin. Pharmacol. *10*, 116–121.

Servant, G., Weiner, O.D., Neptune, E.R., Sedat, J.W., and Bourne, H.R. (1999). Dynamics of a chemoattractant receptor in living neutrophils during chemotaxis. Mol. Biol. Cell *10*, 1163–1178.

Sundaresan, M., Yu, Z.X., Ferrans, V.J., Sulciner, D.J., Gutkind, J.S., Irani, K., Goldschmidt-Clermont, P.J., and Finkel, T. (1996). Regulation of reactive-oxygen-species generation in fibroblasts by Rac1. Biochem. J. *318*, 379–382.

Takemura, Y., Goodson, P., Bao, H.F., Jain, L., and Helms, M.N. (2010). Rac1-mediated NADPH oxidase release of O2- regulates epithelial sodium channel activity in the alveolar epithelium. Am. J. Physiol. Lung Cell. Mol. Physiol. *298*, L509–L520.

Tarpey, M.M., Wink, D.A., and Grisham, M.B. (2004). Methods for detection of reactive metabolites of oxygen and nitrogen: in vitro and in vivo considerations. Am. J. Physiol. Regul. Integr. Comp. Physiol. *286*, R431–R444.

Thomas, E.K., Cancelas, J.A., Chae, H.D., Cox, A.D., Keller, P.J., Perrotti, D., Neviani, P., Druker, B.J., Setchell, K.D., Zheng, Y., et al. (2007). Rac guanosine triphosphatases represent integrating molecular therapeutic targets for BCR-ABL-induced myeloproliferative disease. Cancer Cell *12*, 467–478.

Tirouvanziam, R., Conrad, C.K., Bottiglieri, T., Herzenberg, L.A., Moss, R.B., and Herzenberg, L.A. (2006). High-dose oral N-acetylcysteine, a glutathione prodrug, modulates inflammation in cystic fibrosis. Proc. Natl. Acad. Sci. USA *103*, 4628–4633.

Van Aelst, L., and D'Souza-Schorey, C. (1997). Rho GTPases and signaling networks. Genes Dev. *11*, 2295–2322.

van Zandwijk, N., Dalesio, O., Pastorino, U., de Vries, N., and van Tinteren, H. (2000). EUROSCAN, a randomized trial of vitamin A and N-acetylcysteine in patients with head and neck cancer or lung cancer. For the EUropean Organization for Research and Treatment of Cancer Head and Neck and Lung Cancer Cooperative Groups. J. Natl. Cancer Inst. *92*, 977–986.

Veber, D.F., Johnson, S.R., Cheng, H.Y., Smith, B.R., Ward, K.W., and Kopple, K.D. (2002). Molecular properties that influence the oral bioavailability of drug candidates. J. Med. Chem. *45*, 2615–2623.

Velaithan, R., Kang, J., Hirpara, J.L., Loh, T., Goh, B.C., Le Bras, M., Brenner, C., Clement, M.V., and Pervaiz, S. (2011). The small GTPase Rac1 is a novel binding partner of Bcl-2 and stabilizes its anti-apoptotic activity. Blood *117*, 6214–6226.

Wienken, C.J., Baaske, P., Rothbauer, U., Braun, D., and Duhr, S. (2010). Protein-binding assays in biological liquids using microscale thermophoresis. Nat Commun *1*, 100. 10.1038/ncomms109.

Wind, S., Beuerlein, K., Eucker, T., Müller, H., Scheurer, P., Armitage, M.E., Ho, H., Schmidt, H.H.H.W., and Wingler, K. (2010). Comparative pharmacology of chemically distinct NADPH oxidase inhibitors. Br. J. Pharmacol. *161*, 885–898.

Williams, H.C., and Griendling, K.K. (2007). NADPH oxidase inhibitors: new antihypertensive agents? J. Cardiovasc. Pharmacol. *50*, 9–16.